Journal of Catalysis **197,** 6–16 (2001)
doi:10.1006/jcat.2000.3052, available online at http://www.idealibrary.com on IDEAL®

Mechanism of SO_2 Promotion for NO Reduction with NH_3 over Activated Carbon-Supported Vanadium Oxide Catalyst

Zhenping Zhu,* Zhenyu Liu,*,[1] Hongxian Niu,* Shoujun Liu,* Tiandou Hu,† Tao Liu,† and Yaning Xie†

*State Key Laboratory of Coal Conversion, Institute of Coal Chemistry, Chinese Academy of Sciences, Taiyuan, 030001, People's Republic of China; and †State Key Laboratory of Synchrotron Radiation, Institute of High Energy Physics, Chinese Academy of Sciences, Beijing, 100039, People's Republic of China

Received January 18, 2000; revised August 28, 2000; accepted September 1, 2000

SO_2 shows a significant promoting effect on the activity of V_2O_5/AC catalyst for NO reduction with ammonia at low temperatures (180–250°C). In the present study, the mechanism of the SO_2 promotion was studied. It was found that the promoting effect of SO_2 on the catalytic activity is due to the formation of a sulfate species on the catalyst surface. The sulfate species is linked to carbon surfaces other than vanadium or mineral surfaces. There is a synergetic role between carbon and V_2O_5 for the formation of surface sulfate species. A possible mechanism is proposed. SO_2 is adsorbed and oxidized by oxygen to SO_3 on the vanadium surface, and the formed SO_3 shifts to the carbon surface and converts into sulfate species. The formed sulfate species acts as a new acid site, improves significantly the NH_3 adsorption, and hence promotes the activity of the catalyst. During the reaction in the presence of SO_2 at low temperatures, the sulfate species stays on the catalyst surface, while the ammonium ions react with NO continuously to avoid the formation and deposition of excess ammonium sulfate salts on the catalyst surface.

INTRODUCTION

The emission of nitric oxide (NO) from power plants is a major environmental pollution issue. The most widely adopted method to remove NO from flue gas is the selective catalytic reduction (SCR) of NO with NH_3 according to the following reaction:

$$4NH_3 + 4NO + O_2 \rightarrow 4N_2 + 6H_2O.$$

However, the currently used TiO_2-supported V_2O_5 catalyst must be used at temperatures above 350°C to avoid catalyst deactivation by SO_2 (1). New catalysts that can be used for low-temperatures SCR are needed (2–4). Many previously reported catalysts show high activities for the SCR reaction at 120–250°C (3–8) but are prone to SO_2 deactivation due to the formation of sulfate salts (8, 9).

Recently, we reported an activated carbon (AC)-supported vanadium oxide (V_2O_5/AC) catalyst (10–12), which shows high catalytic activity for the reduction of NO with NH_3 in the temperature range of 180–250°C. More interestingly, SO_2 does not poison the catalyst of low vanadium loadings but greatly promotes its activity. Similar behavior of SO_2 was also reported for V_2O_5/TiO_2-catalyzed SCR reaction at temperatures above 350°C (13, 14). Chen and Yang (15) showed that SO_4^{2-}/TiO_2 exhibits a superacid property and thus a considerable activity for the SCR reaction at temperatures above 400°C.

Previous studies suggested that the promoting effect of SO_2 on the activity of V_2O_5/AC catalyst results from the formation of certain sulfur-containing species on catalyst surface (11, 12). However, some important aspects of the SO_2 promotion mechanism remain unclear. What is the sulfur-containing species? On which site does the sulfur-containing species locate, vanadium or carbon? Are there some changes of the catalyst structure during the SCR reaction in the presence of SO_2? How does the sulfur-containing species promote the SCR reaction? Is it possible that the promoting effect of SO_2 is associated with the existence of alkali metal compounds in the AC? It has been reported (14, 16, 17) that the V_2O_5/TiO_2 catalyst is severely deactivated by alkali metal compounds, such as K_2O, Na_2O, KCl, NaCl, etc., in the absence of SO_2, but the deactivation disappears in the presence of SO_2. Furthermore, why is the V_2O_5/AC catalyst, unlike the V_2O_5/TiO_2 catalyst (1), not deactivated by SO_2 at low temperatures? These issues are studied in the present paper, which is an important step toward understanding both the mechanism of the SO_2 promoting effect on the V_2O_5/AC catalyst and the role of carbon as a catalyst or support in other catalytic systems.

EXPERIMENTAL

Catalyst Preparation

The support, activated carbon (AC), was prepared from a commercial coal-derived semicoke (Datong Coal Gas Co., China) through steam activation at about 900°C. The AC was then oxidized with concentrated HNO_3 at 60°C for 1 h,

[1] To whom correspondence should be addressed. Fax: +86-351-404-1153. E-mail: zyl@public.ty.sx.cn.

0021-9517/01 $35.00

TABLE 1

BET Surface Area[a] and Mineral Content[b] Analyses of Activated Carbon

AC	BET SA (m^2/g)	Total content of minerals (%)	SiO_2	Al_2O_3	Fe_2O_3	CaO	MgO	TiO_2
Original	647	12.24	51.77	23.28	14.07	3.33	4.54	0.92
Oxidized by nitric acid	560	9.33	56.70	25.13	10.75	1.58	2.78	0.69

[a] Measured by N_2 adsorption at 77 K.
[b] Measured by standard coal analysis method.

followed by filtration, washing with distilled water, and drying at 120°C for 5 h. Physical characteristics and the mineral analyses of the AC are presented in Table 1. The V_2O_5/AC catalysts were prepared by pore volume impregnation of the HNO_3-oxidized AC with an aqueous solution of ammonium metavanadate in oxalic acid, followed by overnight drying at 50°C and then at 120°C for 5 h, and by calcination in Ar for 8 h at 500°C and preoxidization in air at 250°C for 5 h.

Presulfation of the Catalyst

In some cases, before activity measurement, the 1 wt% V_2O_5/AC catalyst was presulfated either by (1) 1000 ppm SO_2 in Ar, by (2) 1000 ppm SO_2 and 3.3% O_2 in Ar, or by (3) 2 mol/l H_2SO_4. For SO_2 and $SO_2 + O_2$ treatment, 0.2 g of catalyst was sulfated at a total flow rate of 300 ml/min at 250°C for 2 h, followed by a purge of Ar (200 ml/min) for 1 h to remove the physically adsorbed SO_2 at the same temperature. For the H_2SO_4 treatment, pore volume impregnation was used with an aqueous solution of 2 mol/l H_2SO_4, followed by drying at 110°C for 5 h.

Activity Test

All of the activity tests were carried out in a fixed-bed quartz reactor at 250°C. The catalyst were initially subjected to a reaction mixture, 500 ppm NO, 560 ppm NH_3, 3.3 vol% O_2, and balance Ar, at a space velocity of 90,000 h^{-1} for 4 h to allow a steady-state NO conversion to be reached. A SO_2-containing Ar stream was then fed into the reactor to replace Ar and to maintain the initial concentrations of NO, NH_3, and O_2 and to yield a SO_2 concentration of 400 ppm. The concentrations of NO, NO_2, SO_2, and O_2 at the inlet and the outlet of the reactor were simultaneously monitored by an online flue gas analyzer (KM9006 Quintox, Kane International Limited) equipped with NO, NO_2, SO_2, O_2, and CO sensors.

Procedure of TPD of NH_3

Temperature-programmed desorption (TPD) experiments were performed in the same reactor to determine the effect of SO_2 on the NH_3 adsorption. A 0.1 g amount of 1 wt% V_2O_5/AC catalyst was loaded in the reactor and was pretreated *in situ* in a He stream (50 ml/min) at 500°C for 1 h, and then cooled to 50°C in the same stream. The pretreated sample was then exposed to a gas mixture containing 2000 ppm NH_3 in Ar at a flow rate of 100 ml/min. After an adsorption equilibrium reached (about 1 h), the sample was purged with He of 50 ml/min for 1 h to remove the physically adsorbed NH_3 and Ar. Finally, TPD experiment was carried out in He of 50 ml/min at a heating rate of 10°C/min from 50°C to 500°C. During the TPD, exit NH_3 was continuously analyzed using a TCD detector in an on-line gas chromatograph (GC-17A, Shimadzu). To understand the effect of sulfate species loaded on the V_2O_5/AC catalyst on the NH_3 adsorption, the sample was presulfated before the NH_3 adsorption process (following the 500°C pretreatment of the sample). The presulfation was performed in a gas mixture containing 2000 ppm SO_2 + 3 vol% O_2 in Ar at a flow rate of 100 ml/min and a temperature of 50°C for 2 h, followed by a He purge of 1 h to remove physically adsorbed SO_2. To estimate the intervention of SO_2 signal in the NH_3 signal, TPD of SO_2 was also performed separately following the TPD process for NH_3.

Test of Reactivity of NH_4HSO_4 Deposited on Catalyst Surface

The 1 wt% V_2O_5/AC catalyst was selected to investigate the reactivity of NH_4HSO_4 which may be formed on the catalyst surface at the reaction temperature. NH_4HSO_4 was predeposited by pore volume impregnation of the catalysts with NH_4HSO_4 aqueous solution, followed by overnight drying at 110°C. A 0.2 g amount of NH_4HSO_4-deposited catalyst was exposed to a mixture stream containing about 1000 ppm (or 540 ppm) NO, 3.3 vol% O_2 in Ar, at a total flow rate of 300 ml/min and with programmed heating from 30°C to 480°C at heating rate of 10°C/min. During the reaction, exiting NO and SO_2 were continuously analyzed using the flue gas analyzer, and the amount of NO removed was used to estimate the reactivity of ammonium ions in NH_4HSO_4.

FTIR and XPS Analyses

Fourier transform infrared spectroscopy (FTIR) and X-ray photoelectron spectroscopy (XPS) were used to determine the nature of the sulfur-containing species adsorbed

on the catalyst surface. FTIR spectra of the samples were recorded on a Magna-IR 550-II spectrometer (Nicolet) at ambient temperature. In order to obtain enough strong signals of vanadium species, a catalyst with a V_2O_5 loading of 5 wt% was used here and in the XAFS analyses later, which was based on the fact that this catalyst is also promoted by SO_2, although the promoting effect of SO_2 is more significant for the catalysts with lower V_2O_5 loadings (11). Before the measurement, the 5 wt% V_2O_5/AC catalyst was subjected to a SCR reaction at 250°C in the absence or presence of SO_2 for 10 h. The reaction conditions were the same as those described in the section on the activity test. After the SCR reaction, the catalyst sample was *in situ* purged at 250°C in Ar for 1 h to remove the physically adsorbed SO_2, cooled in Ar to room temperature, and then kept in a sealed vessel. The reacted catalysts were seperately mixed with potassium bromide with a sample-to-potassium bromide ratio of 1 : 10, ground, and pressed into a thin slice. Finally, the prepared sample slice was fitted in the sample chamber and preformed for FTIR analyses.

XPS spectra were measured with a Perkin-Elmer PHI-5300 X-ray photoelectron spectrometer, using Mg$K\alpha$ as the radiation source. The 1 wt% V_2O_5/AC catalyst was presulfated at 250°C in 1000 ppm $SO_2 + 3.3\%$ O_2 in Ar for 2 h or was subjected to a SCR reaction at 250°C in the presence of SO_2 for 10 h. After that, the catalyst sample was *in situ* purged at 250°C in Ar for 1 h to remove the physically adsorbed SO_2, cooled in Ar to room temperature, and then kept in a sealed vessel. The presulfated or reacted catalysts was crushed and pressed into a sample holder on a double-sided glue tape. The preparation chamber was degassed at ca. 1×10^{-6} Torr and maintained at 6×10^{-9} Torr for sample analysis. The charging effect of the sample was calibrated by the C(1*s*) line at 284.6 eV.

XAFS Measurement

The X-ray absorption fine structure (XAFS) technique, including extended X-ray absorption fine structure (EXAFS) and X-ray absorption near-edge structure (XANES), was used to determine the chemical forms of the vanadium species in the V_2O_5/AC catalysts before and after SCR reaction. The 5 wt% V_2O_5/AC catalyst after the SCR reaction in the absence or presence of SO_2 was the same as that used in FTIR analyses. Before the measurement, the sample was crushed into fine particles of less than 200 mesh and coated onto a transparent adhesive tape. The measurements were performed on wiggler beam line 4W1B at the Beijing Synchrotron Radiation Facility (BSRF). A double crystal of Si(111) was used to monochromatize X-rays from the 2.2 GeV electron storage ring with an average ring current of 80 mA. V K-edge absorption spectra were recorded in transmission mode in the range of photon energies from 5265 to 6265 eV at an interval of 0.5 eV in the XANES region and at an interval of 3 eV in the EAXFS region. Fourier transformation was performed on the k^3-weighted EXAFS oscillation in the range of 3–14 $Å^{-1}$.

EDX Elemental Analysis

Energy dispersive X-ray (EDX) analysis was performed on a combined system of a KYKY-1000B scanning electron microscopy (SEM) and a TN5400 X-ray analyzer. The 1 wt% V_2O_5/AC catalyst after the SCR reaction in the presence of SO_2 was used and was the same as the corresponding one used in the XPS analysis. During the EDX analysis, the SEM of the sample was obtained first, which mainly showed the appearance of two types of particles: dark bulk matrix and bright mineral particle. On the basis of the SEM, different areas on the catalyst surface were selected for elemental composition analysis by EDX.

RESULTS AND DISCUSSION

Nature of Sulfur-Containing Species on the Catalyst Surface

Effect of catalyst presulfation. The promoting effect of SO_2 on the activity of 1 wt% V_2O_5/AC catalyst is shown in Fig. la. In the absence of SO_2, the catalystic activity is relatively low under the employed conditions, with a NO removal rate of about 0.2 $\mu mol \cdot s^{-1} \cdot g^{-1}$. When SO_2 is introduced into the feed gas, the catalytic activity increases greatly and reaches a steady-state rate of 0.31 $\mu mol \cdot s^{-1} \cdot g^{-1}$. This clearly indicates that the activity of the V_2O_5/AC catalyst is promoted by SO_2. Our previous paper (11) showed that the promoting effect of SO_2 is not due to

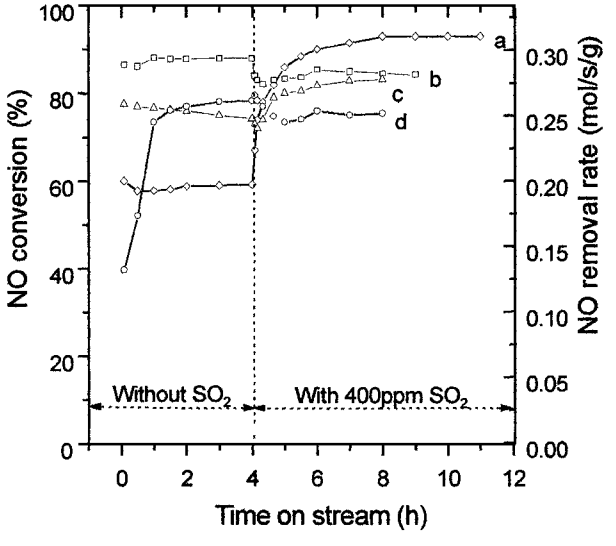

FIG. 1. Effect of presulfation on the activity of 1 wt% V_2O_5/AC catalyst: (a) nontreated; (b) treated by $SO_2 + O_2$; (c) treated by SO_2; (d) treated by H_2SO_4. Reaction conditions: 500 ppm NO, 560 ppm NH_3, 3.3% O_2; temperature, 250°C; WHSV, 90,000 h^{-1}.

gas-phase SO_2 but is associated with the formation of certain sulfur-containing species on the catalyst surface.

The effects of the presulfations are illustrated in Figs. 1b–1d. In the absence of SO_2, the catalysts pretreated by SO_2, $SO_2 + O_2$, and H_2SO_4 show higher steady-state activity than the untreated sample. The activity of the catalyst treated by H_2SO_4 is initially low but increases quickly with time. This may be due to some H_2O remaining on the catalyst surface after the H_2SO_4 treatment. The competitive adsorption of H_2O and NH_3 (13) reduces NH_3 coverage on the catalyst surface and subsequently reduces the reaction rate. The adsorbed H_2O may be removed by evaporation, which hence results in an increased reaction rate. Interestingly, the $SO_2 + O_2$ treatment is more conducive to activity improvement than the SO_2 treatment. When SO_2 is introduced into the feed, the activities of the catalysts treated by $SO_2 + O_2$ and H_2SO_4 show a slight decline, while the activity of the catalyst treated by SO_2 shows an obvious increase.

These observations suggest that O_2 is important for SO_2 adsorption and the activity improvement. As is well known, V_2O_5 is an effective catalyst for SO_2 oxidation. Therefore, the adsorbed SO_2 on the surface of V_2O_5/AC catalyst may be in a form of S^{6+}, such as SO_3 and SO_4^{2-}; of these, SO_4^{2-} seems to be more reasonable because H_2O is formed during the NO–NH_3–O_2 reaction, which can cause SO_3 to convert into SO_4^{2-} ion. It should be pointed out that during the reaction without SO_2, the increased activity of the catalyst treated by SO_2 may result from SO_2 adsorption during the treatment and subsequent oxidation by O_2 during the NO–NH_3–O_2 reaction. Note that if the promoting effect of SO_2 is due to the formation of surface sulfate species, all the catalysts presented in Fig. 1 should eventually reach the same steady state in the presence of SO_2, regardless of the pretreatment. However, the experimental results show that the pretreatments have different influences on the catalytic activity in the presence of SO_2. As described below, the promoting effect of SO_2 surely results from the formation of surface sulfate species. The activity changes deriving from the pretreatment have not been clearly explained here but may be associated with the somewhat irreversible changes in catalyst structure during the pretreatment since the pretreatment conditions are obviously different from the reaction conditions after all.

XPS characterization. The 1 wt% V_2O_5/AC catalysts after $SO_2 + O_2$ presulfation and the SCR reaction in the presence of SO_2 were measured for XPS spectra. The signals of V(2*p*) for both of the samples are very weak, possibly due to the low vanadium content in the catalysts. The S(2*p*) and O(1*s*) spectra are shown in Fig. 2. The S(2*p*) spectra of both samples exhibit a single peak with a binding energy of 168.5 eV. It is attributed to S^{6+} species such as sulfate in Na_2SO_4, $FeSO_4$, and $Fe_2(SO_4)_3$ (18). The O(1*s*) spectra of the reacted and sulfated samples show a main peak at 532.0 and 533.0 eV, respectively. Both of the spectra are

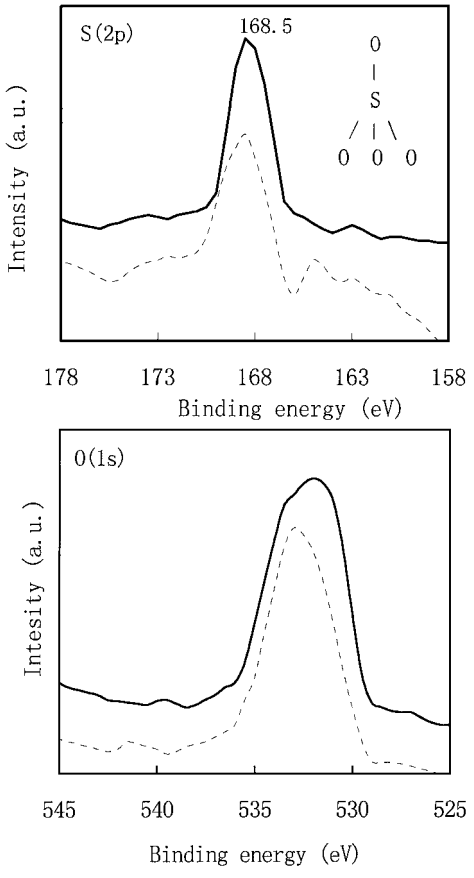

FIG. 2. S(2*p*) and O(1*s*) XPS spectra of the 1 wt% V_2O_5/AC catalysts after $SO_2 + O_2$ treatment (solid lines) or SCR reaction in the presence of SO_2 (dashed lines).

very wide, with a half-height width above 4.2 eV. This is associated with complicated circumstances related to oxygen. As expected, there are metal oxides (oxides of V, Si, Al, Fe, etc.), carbon–oxygen functional groups, and sulfur–oxygen species in the catalysts. The binding energy of O(1*s*) in metal oxides is in the range of 529.3–531.6 eV, and that in carbon–oxygen is over 533 eV (18, 19). However, the main peaks of the present samples, located at 532–533 eV, are attributed to sulfate oxygen (18). Therefore, the XPS results lead to the conclusion that the sulfur-containing species on the V_2O_5/AC catalysts surface is sulfate.

FTIR characterization. Figure 3 shows the FTIR spectra of the 5 wt% V_2O_5/AC catalysts before and after the SCR reaction in the absence or presence of SO_2, along with the spectrum of the AC. No absorption signal is found for the AC under the analysis conditions. The spectrum of the 5 wt% V_2O_5/AC catalyst before the SCR reaction shows a very broad band in the range of 1000–1220 cm^{-1} and peaked at 1087 cm^{-1}, which may be associated with the stretching frequency of $V^{5+}{=}O$. This assignment is similar to but noticeably difference from previous reports (20–22). Frederickson and Hausen (20) showed that the stretching

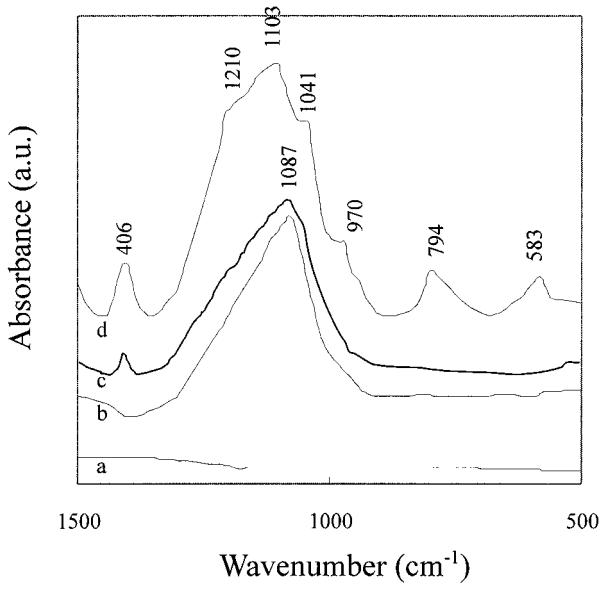

FIG. 3. FTIR spectra of the AC and the 5 wt% V_2O_5/AC catalysts before and after SCR at 250°C: (a) AC; (b) fresh 5 wt% V_2O_5/AC; (c) 5 wt% V_2O_5/AC after SCR reaction in the absence of SO_2; (d) 5 wt% V_2O_5/AC after SCR reaction in the presence of SO_2.

vibration of $V^{5+}=O$ occurs at about 1020 cm^{-1} for bulk V_2O_5. Inomata *et al.* (21) found that the stretching vibration is not influenced by supporting V_2O_5 on TiO_2. Tarama *et al.* (22) showed that V_2O_5 supported on γ-Al_2O_3 and SiO_2 exhibit a sharp absorption at 1023 cm^{-1}. The broad band of the present catalyst possibly results from the lowered symmetry of vanadium species or the existence of some different species.

After a SCR reaction in the absence of SO_2, the V_2O_5/AC catalyst exhibits similar bands in the range of 1000–1220 cm^{-1} and a new absorption band at about 1406 cm^{-1}, which can be assigned to NH_4^+ species chemically adsorbed on Brønsted acid sites during the SCR reaction (15, 23, 24). After a SCR reaction in the presence of SO_2, the V_2O_5/AC catalyst shows a very complex spectrum, which involves several bands at 583, 794, 970, 1041, 1103, 1210, and 1406 cm^{-1}. The band at 1406 cm^{-1} significantly increases in intensity compared to that after reaction in the absence of SO_2, indicating that the presence of SO_2 in the reaction stream results in an increase in the formation of surface NH_4^+ ions. The bands at 1103 and 583 cm^{-1} may be attributed to the characteristic frequencies of the SO_4^{2-} ion. Free SO_4^{2-} ion has a T_d symmetry and shows two infrared-active peaks at 1104 (ν_1) and 613 cm^{-1} (ν_2) (25). When SO_4^{2-} is bound to the catalyst surface, its symmetry can be lowered to C_{3v} or C_{2v}. The ν_1 band splits into two peaks for C_{3v} symmetry and splits into three peaks for C_{2v} symmetry (25). The bands at 970 and 1210 cm^{-1} may result from the lowered symmetry of sulfate species from T_d to C_{2v} and then the ν_1 splitting. A similar observation and suggestion were given by Chen and Yang (15) for the sulfate species on titania surface. The band at 1041 cm^{-1} may be associated with a $V^{5+}=O$ stretching vibration, which was usually observed at about 1020 cm^{-1} on the TiO_2 surface. The band at 794 cm^{-1} is seldom observed by IR. A similar band existed in the Raman spectra of V_2O_5/TiO_2 catalyst reported by Amiridis *et al.* (13), but the assignment is unclear still.

Sites Linked to Sulfate Species

XAFS characterization. As shown above, the sulfur-containing species, formed during the SCR reaction in the presence of SO_2, exists in sulfate form. It is important to clarify which site is linked to the sulfate species, vanadium or activated carbon. If the sulfate species is linked to the vanadium site, it is possible that the vanadium species is converted into new chemical forms such as $VOSO_4$. To criticize this conjecture, the analyses of XRD and XAFS were performed on 5 wt% V_2O_5/AC catalysts before and after the SCR reaction in the presence of SO_2. However, the profiles of XRD for both samples show no signal for vanadium species due to their small particle size. On the other hand, XAFS analyses provide a clear result.

The V K-edge X-ray absorption near-edge structures (XANES) of the 5 wt% V_2O_5/AC catalysts before and after SCR reaction in the presence of SO_2 are shown in Fig. 4, in which the XANES spectra of V_2O_5 and $VOSO_4 \cdot 4H_2O$ are also shown. Vanadium in V_2O_5 is in C_s symmetry with five

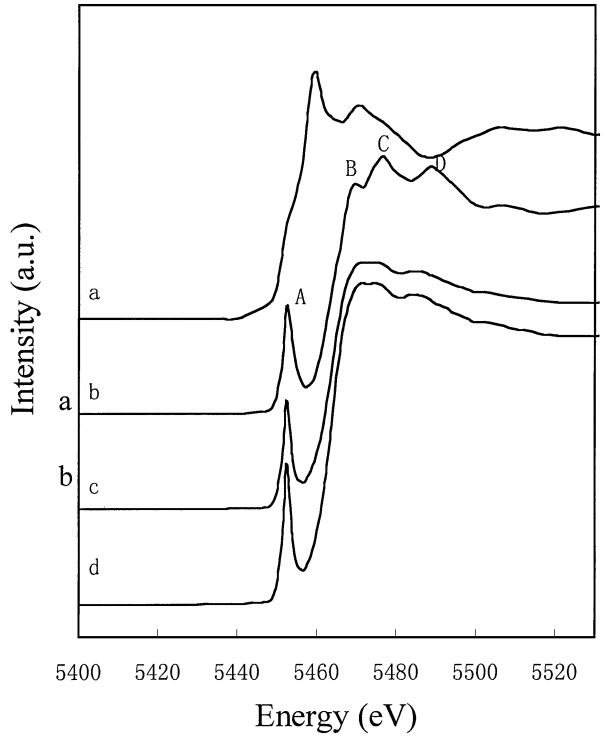

FIG. 4. V K-edge XANES of $VOSO_4$ (a), V_2O_5 (b), and 5 wt% V_2O_5/AC catalysts before (c) and after (d) the SCR reaction in the presence of SO_2.

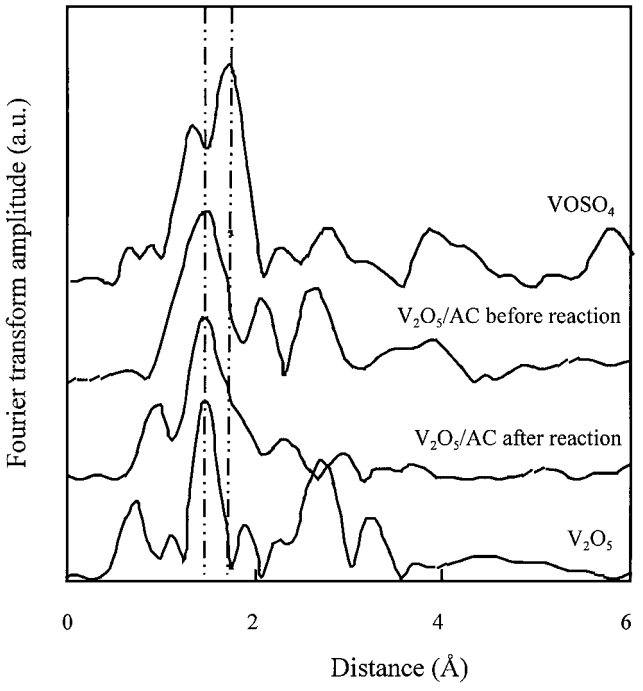

FIG. 5. V K-edge EXAFS RSF of 5 wt% V_2O_5/AC catalysts and some reference compounds.

coordinated oxygen atoms. Its XANES shows a strong pre-edge absorption (structure A), which is related to a $1s \rightarrow 3d$ forbidden transition caused mainly by mixing of the $2p$ orbital of oxygen with the $3d$ orbital of vanadium in the terminal V=O group (26–28). On the other hand, vanadium in $VOSO_4 \cdot 4H_2O$ is in C_{4v} symmetry with six coordinated oxygen atoms, and its XANES shows a weak pre-edge absorption (26, 29), which is in agreement with the present observation that $VOSO_4 \cdot 4H_2O$ exhibits a very weak structure A. In addition, the structure B in $VOSO_4 \cdot 4H_2O$, attributed to the $1s \rightarrow 4p$ transition, is much sharper and located at a lower energy than that in V_2O_5. Following the structure B, both C and D structures exist for V_2O_5, while only the C structure exists for $VOSO_4$ and shifts to lower energy.

The XANES features of the two catalyst samples are rather similar. They are very different from that of $VOSO_4 \cdot 4H_2O$, but similar to that of V_2O_5, although they exhibit weaker B, C, and D structures than crystalline V_2O_5, possibly due to the small particle size of vanadium species in the catalysts.

Figure 5 shows the radial structural functions (RSF) of the two catalyst samples, $VOSO_4 \cdot 4H_2O$ and V_2O_5, obtained by the Fourier transform of k^3-weighted EXAFS following standard analysis (30). Note that all the data in the RSF spectra are presented without any correction for phase shift, and hence the distance indicated along the abscissa does not represent the true distance between vanadium and neighboring atoms. The peaks appearing at 1–2 Å are associated with V–O bonds, and the peaks appearing at 2–3 Å show the presence of neighboring vanadium atoms. The RSF of $VOSO_4 \cdot 4H_2O$ is very different from that of V_2O_5. The former shows double peaks at 1.3 and 1.7 Å for the V−O shell, which may correspond to the short V=O double bond and the longer V−O single bonds, respectively (26, 31). On the other hand, the RSF of V_2O_5 exhibits a single peak for the V−O shell at 1.48 Å and a strong peak for the V−V shell at about 2.7 Å.

Both of the V_2O_5/AC catalysts show a peak at 1.48 Å for the V−O shell, which is clearly similar to that of V_2O_5 rather than that of $VOSO_4 \cdot 4H_2O$. In addition, the V−V peak at 2.7 Å can be seen in the RSF of the catalyst before reaction as in the case of V_2O_5, suggesting that the dominant surface vanadium species are dimeric or polymeric. But the height of the V–V peak is lower than that for V_2O_5, showing that the number of neighboring vanadium atoms is smaller than that in the V_2O_5 crystal. On the other hand, the catalyst after reaction shows no peak above the noise level at longer distances (>2 Å), suggesting that the dominant surface vanadium species are isolated from each other.

In conclusion, the vanadium species in the V_2O_5/AC catalyst is dimeric or polymeric V_2O_5. During the SCR reaction in the presence of SO_2, the chemical form of the vanadium species does not change, although the particle sizse of the vanadium species seems to be getting small.

EDX elemental analysis. As revealed by XAFS characterization, $VOSO_4$ is not formed during the SCR reaction in the presence of SO_2. However, it is possible for sulfate species to link to the vanadium surface by physical or chemical adsorption. To examine this, after the SCR reaction in the presence of SO_2, the 1 wt% V_2O_5/AC catalyst was analyzed by the EDX technique. Table 2 presents the elemental

TABLE 2

EDX Elemental Analyses of the 1 wt% V_2O_5/AC Catalyst after Reaction in the Presence of SO_2 (atom %)

Area mark	S	V	Si	Al	Fe	S/V	Type of area
A	40.25	7.3	39.13	12.79	0.52	5.51	Average
B	80.24	17.55	1.79	0.00	0.42	4.57	Matrix
C	53.77	7.39	26.57	12.26	0.00	7.28	Matrix
D	57.56	11.88	18.47	12.09	0.00	4.85	Matrix
E	84.47	14.62	0.91	0.00	0.00	5.78	Matrix
F	61.12	21.21	16.43	0.00	1.24	2.88	Matrix
G	42.59	7.43	30.74	19.24	0.00	5.73	Matrix
H	78.02	3.32	12.21	5.43	1.02	23.5	Matrix
I	79.04	0.00	19.84	1.12	0.00	NVD[a]	Matrix
J	73.7	0.00	20.73	5.57	0.00	NVD	Matrix
K	0.00	21.86	10.43	57.17	10.54	0.00	Matrix
L	0.00	0.00	64.8	35.2	0.00	NVD	Mineral
M	1.95	5.45	20.93	64.62	7.05	0.35	Mineral
N	32.75	1.67	63.39	2.19	0.00	19.6	Mineral
O	13.46	0.00	86.54	0.00	0.00	NVD	Mineral
P	3.23	0.00	96.23	0.54	0.00	NVD	Mineral

[a] NVD = no vanadium detected in the analysis-limiting range.

compositions of different areas (marked A–P) on the catalyst surface. The data of area A represent an average elemental composition measured in a large highlighted area. It shows that the catalyst surface contains a large amount of sulfur, with a S/V mole ratio of 5.51. The areas B–P represent partial and local results of small highlighted areas; among them, the areas B–K represent the bulk matrix of catalyst surface, while the areas L–P represent some mineral particles.

It is clear that the S/V ratios are not uniform throughout the surface. The S/V ratios of areas B–G are in the range of 2–8, which is of the same order of magnitude as the average value. Unlike this, the values of areas H–J are very high, especially at areas I and J, which show no vanadium atom but a rather high sulfur content. In contrast, area K shows no sulfur atom but a high vanadium content. These results clearly indicate that the sulfate species, formed on the V_2O_5/AC catalyst surface, is not linked to the vanadium species. This is in agreement with the suggestion of XAFS analyses. Therefore, it is believed that the sulfate species is linked to the AC surface.

In a way similar to that described above, Table 2 also shows that there is no correlation between sulfur atom and Si, Al, and Fe atoms. Although some other metals that may exist in the AC, such as Mg, Ca, Na, K, etc., were not detected due to low concentrations, it is expected that their concentrations are too low to capture all the sulfate species. This seems to indicate that the sulfate species, formed during the SCR reaction in the presence of SO_2, is mainly linked to the carbon surface.

Furthermore, as previously reported (14, 16, 17) for V_2O_5/TiO_2 catalyst, very low contents of alkali metal compounds, such as K_2O, Na_2O, KCl, NaCl, K_2SO_4, etc., can severely poison the catalyst in the absence of SO_2, and the poisoning effect vanishes in the presence of SO_2. Therefore, one can question that for the V_2O_5/AC catalyst, the alkali metal compounds that may exist in the AC might result in a low catalytic activity in the absence of SO_2, and the effect of SO_2 might be virtually to recover the activity. This question is answered by performing some special experiments as follows.

Effect of demineralization of AC on the SO_2 promotion. The AC was demineralized by both HCl acid and mixed HCl–HF acid. These treatments can effectively remove alkali or alkali-earth metal compounds that may exist in the AC. The resulting ACs were analyzed by ICP and showed no existance of alkali or alkali-earth metals within analysis errors. Using the demineralized ACs, 1 wt% V_2O_5/AC catalysts were prepared and tested for the effect of SO_2 on their activities. The results are shown in Fig. 6, in comparison with that of the catalyst prepared from the original (non-demineralized) AC.

In the absence of SO_2, the catalysts prepared from the demineralized AC show relatively lower activities than that of the catalyst prepared from the original AC. When SO_2 is introduced into the feed, the activities increase gradually with time and reach a steady state, which is roughly similar to the behavior of the catalyst prepared from the original AC. The differences in the behaviors of the three catalysts are due to possible changes in the structure of the AC caused by the demineralizations. Following the reactions shown in Fig. 6, the three catalysts are heated separately with the temperature-programmed method, and the released SO_2 is detected. The result is presented in Fig. 7. It is found that the three catalysts exhibit similar SO_2 desorption with a peak at about 345°C, although the desorbed SO_2 amounts are different due to the possible change of the AC structure. These results clearly indicate that the promoting effect of SO_2 is associated not with alkali or alkali-earth metals in the AC but with the interaction between the formed sulfate species and carbon.

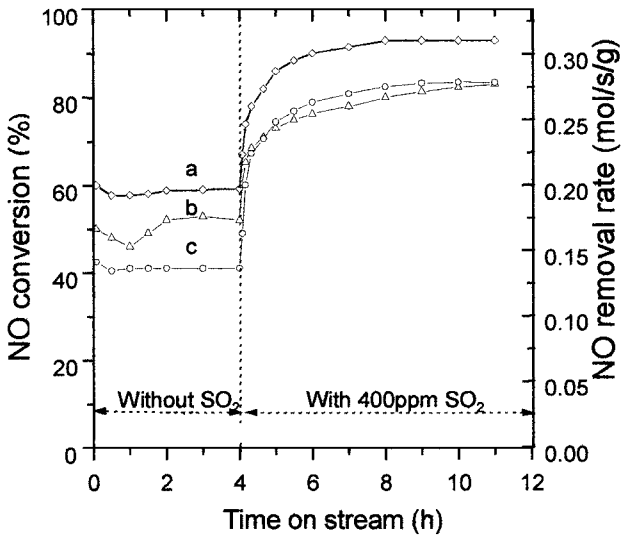

FIG. 6. Effect of SO_2 on the activities of the 1 wt% V_2O_5/AC catalysts prepared from original AC (a), HCl-demineralized AC (b), and HCl–HF-demineralized AC (c). Reaction conditions: 500 ppm NO, 560 ppm NH_3, 3.3% O_2, 400 ppm SO_2 (when used); temperature, 250°C; WHSV, 90,000 h^{-1}.

Role of Vanadium on the Formation of the Sulfate Species

As mentioned above, the promoting effect of SO_2 on the activity of V_2O_5/AC catalyst is due to the formation of sulfate species on the carbon surface. This is in agreement with the previous observations (11, 12) that the promoting effect of SO_2 is found only for the catalysts with low V_2O_5 loading (1–5 wt%), and that the promotion level declines with increasing V_2O_5 loading. However, our previous reports (10–12) showed that the promoting effect of SO_2 is not found for the AC (no V_2O_5 loading). In addition, unlike the 1 wt% V_2O_5/AC catalyst, the AC shows very little SO_2 desorption after the SO_2-presented SCR reaction (12).

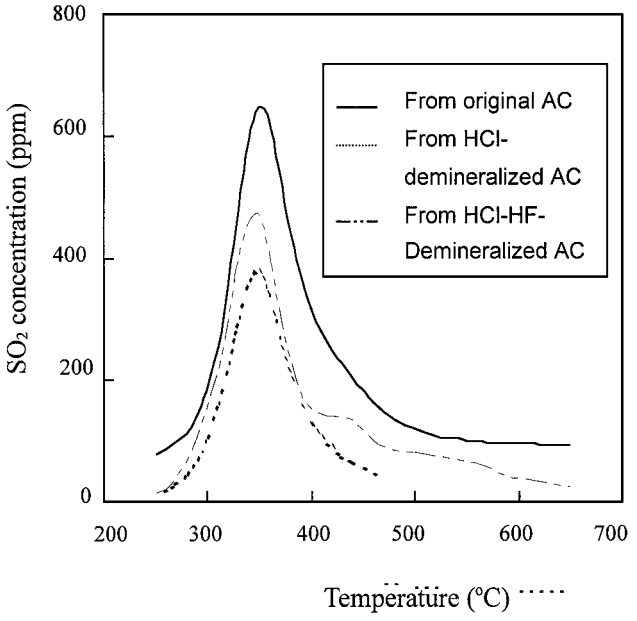

FIG. 7. TPD patterns of SO_2 on the 1 wt% V_2O_5/AC catalysts prepared from different support AC after the SCR reactions shown in Fig. 6. Carrier gas, Ar at 300 ml/min; heating rate, 10°C/min.

These observations suggest that V_2O_5 also plays an important role in the formation of sulfate species.

Figure 8 shows the profiles of temperature-programmed desorption (TPD) of SO_2 adsorbed on the AC, V_2O_5, and the 1 wt% V_2O_5/AC catalysts during oxidation of SO_2 by O_2. It is found that SO_2 adsorption is very limited on the V_2O_5 surface under the adsorption conditions; nearly no SO_2 is desorbed during the TPD from 250°C to 640°C. The TPD of SO_2 for the AC catalyst shows a peak at about 340°C, but the amount desorbed is very low (0.014 mmol/g). The 1 wt% V_2O_5/AC catalyst exhibits a desorption peak at a temperature similar to that for the AC, which gives further support to the suggestion that the formed sulfate species is mainly associated with the carbon surface rather than the vanadium surface. Furthermore, interestingly, the amount desorbed from the 1 wt% V_2O_5/AC catalyst is 0.15 mmol/g, which is about 10 times that for the AC. These observations suggest that there is a synergistic interaction between carbon and V_2O_5 for SO_2 adsorption and the formation of surface sulfate species.

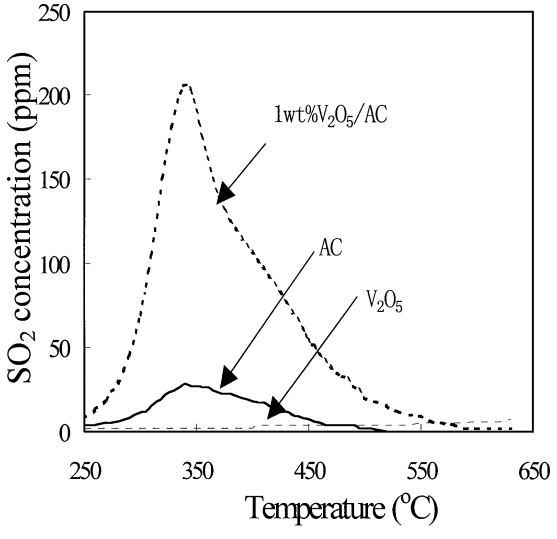

FIG. 8. TPD patterns of SO_2 on different catalysts after oxidation of SO_2 by O_2. The SO_2 oxidation is performed at 250°C in an Ar stream containing 1000 ppm SO_2 and 3.3% O_2 for enough time to allow SO_2 saturation, followed by a purge with Ar for 1 h. The TPD is carried out in an Ar stream of 300 ml/min at a heating rate of 10°C/min.

It was shown in the literature (32, 33) that the SO_2 oxidation reaction on the carbon surface occurs between the adsorbed SO_2 and O_2 is limited by the SO_2 adsorption step. This suggests that SO_2 prefers to be adsorbed and oxidized on the carbon surface at low temperatures, such as room temperature. At higher temperatures, SO_2 adsorption decreases greatly as observed in Fig. 8. On the other hand, SO_2 adsorption on V_2O_5 in the presence of O_2 follows a mechanism in which SO_2 is first oxidized by V_2O_5 and then adsorbed as SO_3, in which the role of O_2 is to reoxidize the reduced vanadium to V_2O_5. But this process needs high temperatures (above 420°C); SO_2 adsorption is very limited at lower temperatures (34) as shown in Fig. 8 (the adsorption is performed at 250°C). Therefore, the increased adsorption of SO_2 on the V_2O_5/AC catalyst under the conditions used results from a synergistic interaction between carbon and V_2O_5, in which SO_2 may first be oxidized into SO_3 on the V_2O_5 surface, and then SO_3 shifts to and stores at the carbon surface. Furthermore, during the SCR reaction the adsorbed SO_3 converts into sulfate species by reacting with H_2O (formed during the SCR reaction). In this mechanism, V_2O_5 acts as an "opening door," and carbon as a "store room" for SO_2 adsorption and sulfate species occupation.

NH_3 Adsorption Improved by Sulfate Species

The normalized TPD profiles of NH_3 adsorbed on the 1 wt% V_2O_5/AC catalyst and the presulfated one are shown in Fig. 9, in which the TPD profile of SO_2 after the presulfation is also shown to facilitate the estimation of the amount of NH_3 desorbed under the intervention of the SO_2 signal. NH_3 desorption on the 1 wt% V_2O_5/AC catalyst exhibits two divided peaks, centered at about 110°C (LT) and 375°C (HT), suggesting that there are at least two distinct NH_3 species on the catalyst surface. They might be somewhat associated with the ammonium ions adsorbed on Brønsted acid V^{5+}–OH sites and the molecularly adsorbed ammonia through a Lewis-type interaction on coordinatively unsaturated cations, respectively, as are well identified by IR spectroscopy for other vanadia-based catalysts (23, 35–38). Rajadhayaksha and

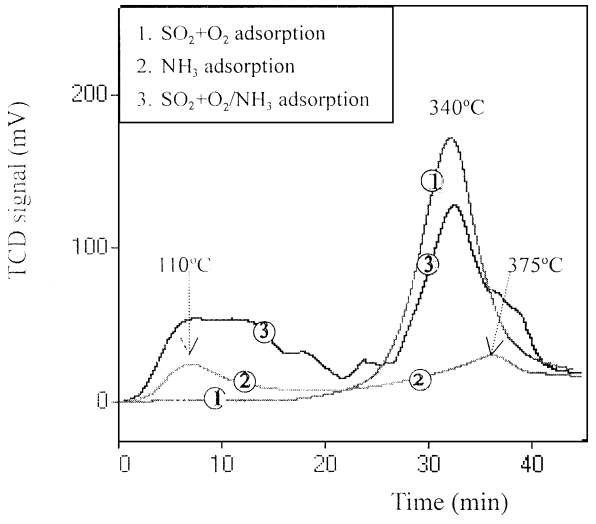

FIG. 9. Normalized TPD profiles of NH_3 (or SO_2) adsorbed on the 1 wt% V_2O_5/AC catalyst after (1) $SO_2 + O_2$ adsorption, (2) NH_3 adsorption, and (3) successive $SO_2 + O_2$ and NH_3 adsorption. TPD conditions: temperature range, 50–500°C; heating rate, 10°C/min; chromatography carrier gas, He at 50 ml/min.

Knäzinger (38) showed by FTIR that the Lewis-type NH_3 species is thermally more stable than the ammonium ion. SO_2 desorption after the presulfation of the catalyst occurs in the range of 270–400°C, peaked at about 340°C, which is similar to the SO_2 desorption profiles after both the SCR reaction and SO_2–O_2 sulfation for the 1 wt% V_2O_5/AC catalyst as shown in Figs. 7 and 8, respectively. More interestingly, the presence of surface sulfate species significantly changes the TPD profile of NH_3 adsorbed on the 1 wt% V_2O_5/AC catalyst (the peak at 340°C is attributed to the SO_2 release). The LT peak greatly increases and some new peaks appear in the higher temperature region, while the HT peak exists as a shoulder due to the strong SO_2 signal and maintains a similar intensity. These results suggest that the sulfate species on the catalyst surface significantly improve the surface acidity (provide new Brønsted acid sites) and then increase and stabilize the surface NH_3 species. It should be pointed out that the SCR reaction is performed at 250°C, at which some of the NH_3 species enhanced by the formation of sulfate species are not stable and might be not involved in the SCR reaction. However, the FTIR analyses shown in Fig. 3 indicate that at the reaction temperature of 250°C, the formation of sulfate species significantly increases the amount of the surface NH_4^+ species. Therefore, it is believed that the surface NH_4^+ species enhanced and stabilized by the sulfate species is associated with the SO_2 promoting effect on the activity of the V_2O_5/AC catalyst.

Additionally, the NH_3 amounts desorbed are 0.89 and 2.21 mmol/g for the free catalyst and the sulfate species covered catalyst, respectively, which are somewhat higher than that for the vanadium amount (0.11 mmol/g) in the catalyst. This suggests that both adsorbed NH_3 and sulfate species are dominantly linked to the carbon surface, although an adsorption on the vanadium sites is also possible. The latter is in line with the results obtained by EXAFS and EDX analyses.

Reactivity of NH_4HSO_4 Deposited on Catalyst Surface

As mentioned above, sulfate species formed on the V_2O_5/AC catalyst significantly improve ammonia adsorption. It is believed that the sulfate and ammonia species exist as ammonium sulfate salts, especially during the SCR reaction in the presence of SO_2, in which H_2O is formed (or exists in flue gas). As reported previously for the V_2O_5/TiO_2 catalysts (1), the formed ammonium sulfate salts such as NH_4HSO_4 and $(NH_4)_2S_2O_7$ may plug the catalyst pore structure and hence deactivate the catalyst at low temperatures (<330°C). However, the previous studies (10, 11) showed that the V_2O_5/AC catalyst is rather stable in the presence of SO_2 at low temperatures (180–250°C). A possible reason is that ammonium sulfate salts formed on the V_2O_5/AC catalyst can react with NO and then be removed from the catalyst surface. This conjecture is supported by the result presented below.

Figure 10 shows the temperature-programmed reaction of NO and NH_4HSO_4 predeposited on the 1 wt% V_2O_5/AC catalyst, in which the change in the NO concentration is used to express the reaction process and the reactivity of NH_4HSO_4, and SO_2 release during the process is also shown. The reaction of NO and ammonium ions starts slowly at about 120°C, and dominantly at about 180°C, and gets faster with increasing temperature. (Note that the

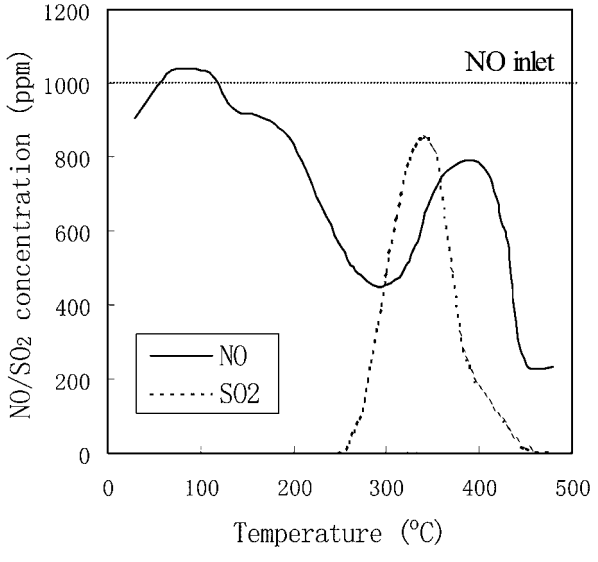

FIG. 10. Temperature-programmed reaction of NO with NH_4HSO_4 deposited on the 1 wt% V_2O_5/AC (solid line) and released SO_2 (dashed line) during the process. Reaction conditions: 1000 ppm NO, 3.3% O_2; total flow rate, 300 ml/min; catalyst amount, 0.2 g.

quick decrease of NO concentration at temperatures above 390°C may result from the reaction of NO with CO (or carbon), which is based on an observation that at temperatures above 360°C the concentrations of O_2 and CO quickly decrease and increase, respectively, with increasing temperature.) This result clearly indicates that the ammonium ion in ammonium sulfate salts on the V_2O_5/AC surface can react with NO at low temperatures. Interestingly, the SO_2 release during the reactions starts at about 260°C, which is much higher than the dominant starting temperature (180°C) of the reaction of NO and the deposited NH_4HSO_4. Therefore, it is believed that during the SCR reaction on the V_2O_5/AC catalyst in the presence of SO_2 at 180–250°C, the formed sulfate species stays on the catalyst surface and acts as new acid site for NH_3 adsorption and activation. At the same time, the ammonium ion reacts continuously with NO to avoid the formation and deposition of excess ammonium sulfate salts on the catalyst surface. Such a process effectively ensures that the V_2O_5/AC catalyst will be promoted but not poinsoned by SO_2 (10–12).

It should be pointed out that the reactivity of NH_4HSO_4 deposited on the V_2O_5/AC catalyst surface is highly dependent on V_2O_5 loading; high V_2O_5 loadings result in a low reactivity of NH_4HSO_4. About this, a systematic study has been done and the results are available in Ref. (39). Additionally, since the reactivity of NH_4HSO_4 on the V_2O_5/AC catalyst is studied here by depositing NH_4HSO_4 on the catalyst via impregnation, one might question whether NH_4^+ and HSO_4^- ions are possibly separated from each other on the catalyst surface. NH_4HSO_4 exists as aquated ions of NH_4^+ and HSO_4^- during the impregnation but turn into microcrystal or amorphous states on the catalyst surface after water evaporation via drying. On the other hand, it is also possible that NH_4^+ and HSO_4^- ions exist separately on the catalyst surface due to some interaction with different surface sites. It is difficult to distinguish between these two situations (the sample with deposited NH_4HSO_4 was analyzed by XRD, but no imformation was obtained). However, a previous study (39) showed that the temperature-programmed decomposition pattern of the deposited NH_4HSO_4 is quite similar to that of the NH_4HSO_4 actually formed during the SCR reaction, suggesting that the reactivity of the deposited NH_4HSO_4 can reflect the actual situation of NH_4HSO_4 formed during the SCR reaction to a certain extent.

CONCLUSIONS

Based on the previous observations that the V_2O_5/AC catalyst is not poisoned but promoted by SO_2 in the NO reduction with ammonia at low temperatures (180–250°C), the mechanism of the SO_2 promotion and the nature of the catalyst stability in the presence of SO_2 are studied in this work. Some conclusions can be drawn as follows:

(1) XPS and FTIR measurements show that the promoting effect of SO_2 on the catalytic activity is due to the formation of sulfate species on the catalyst surface.

(2) XAFS, EDX, and the demineralization experiments of the AC suggest that the form of the vanadium species is not changed before and after the SCR reaction in the presence of SO_2, and that the sulfate species is linked to the carbon surface rather than the vanadium or mineral surfaces.

(3) There is a synergistic role between the carbon and V_2O_5 for SO_2 adsorption and the formation of surface sulfate species. A possible mechanism proposed is that SO_2 is adsorbed and then oxidized by oxygen to SO_3 on the vanadium surface; the formed SO_3 migrates to the carbon surface and then converts to sulfate species through reaction with H_2O.

(4) The formed sulfate species acts as new acid sites, improves significantly NH_3 adsorption, and hence promotes the SCR activity of the catalyst.

(5) During the SCR reaction on the V_2O_5/AC catalyst in the presence of SO_2 at temperatures of 180–250°C, the formed sulfate species stay on the catalyst surface, while the ammonium ions react with NO continuously to avoid the formation and deposition of excess ammonium sulfate salts on the catalyst surface, which effectively results in the V_2O_5/AC catalyst being promoted but not poisoned by SO_2.

ACKNOWLEDGMENTS

The authors gratefully acknowledge the experimental support of Beijing Synchrotron Radiation Laboratory and the financial support from the Natural Science Fundation China (29633030, 29876046), the Shanxi Natural Science Fundation, and Chinese Academy of Sciences.

REFERENCES

1. Bosch, H., and Janssen, F., *Catal. Today* **2**, 369–531 (1988).
2. Jang, B. W. L., Spivey, J. J., Kung, M. C., and Kung, H. H., *Energy Fuels* **11**, 299–306 (1997).
3. Singoredjo, L., Korver, R., Kapteijn, F., and Moulijn, J., *Appl. Catal. B* **1**, 297–316 (1992).
4. Singoredjo, L., Slagt, M., Van Wees, J., Kapteijn, F., and Moulijn, J., *Catal. Today* **7**, 157–165 (1990).
5. Okazaki, S., Kuroha, H., and Okuyama, T., *Chem. Lett.* 45–48 (1985).
6. Grzybek, T., and Papp, H., *Appl. Catal. B* **1**, 271–283 (1992).
7. Nishijima, A., Kiyozumi, Y., Ueno, A., and Kurita, M., *Bull. Chem. Soc. Jpn.* **52**, 3724–3727 (1979).
8. Zhu, Z. P., Liu, Z. Y., Liu, S. J., and Niu, H. X., *Appl. Catal. B* **26**, 25–35 (2000).
9. Kijlstra, W. S., Biervlet, M., Poels, E. K., and Bliek, A., *Appl. Catal. B* **16**, 327–337 (1998).
10. Zhu, Z. P., Liu, Z. Y., Liu, S. J., and Niu, H. X., *Appl. Catal. B* **23**, L229 (1999).
11. Zhu, Z. P., Liu, Z. Y., Liu, S. J., and Niu, H. X., *J. Catal.* **187**, 245–248 (1999).
12. Zhu, Z. P., Liu, Z. Y., Liu, S. J., and Niu, H. X., *Sci. China* **43**, 51–57 (2000).
13. Amiridis, M. D., Wachs, I. E., Deo, G., Jehng, J. M., and Kim, D. S., *J. Catal.* **161**, 247–253 (1996).

14. Chen, J. P., and Yang, R. T., *J. Catal.* **125**, 411–420 (1990).
15. Chen, J. P., and Yang, R. T., *J. Catal.* **139**, 277–288 (1993).
16. Yoshida, H., Takahashi, K., Sekiya, Y., Morokawa, S., and Kurita, S., *in* "Proceeding of the 8th International Congress on Catalysis, Berlin, 1984," Vol. 3, p. 649. Dechema, Frankfurt-am-Main, 1984.
17. Kasaoka, S., Sasaoka, E., and Nanba, H., *Nippon Kagaku Kaishi*, 486 (1984).
18. Wagner, C. D., Riggs, W. M., Davis, L. E., and Moulder, J. F., *in* "Handbook of X-ray Photoelectron Spectroscopy" (G. E. Muilenberg, Ed.), pp. 42–57. Perkin-Elmer Corp., Eden Prairie, MN, 1979.
19. Wagner, C. D., *in* "Practical Surface Analysis (D. Briggs and M. D. Seah, Eds.), 2nd Ed., p. 599. Wiley, Chichester, UK, 1979.
20. Frederickson, L. D., Jr., and Hausen, D. M., *Anal. Chem.* **35**, 818 (1963).
21. Inomata, M., Mori, K., Miyamoto, A., Ui, T., and Murakami, Y., *J. Phys. Chem.* **87**, 754 (1983).
22. Tarama, K., Yoshida, S., Ishida, S., and Kakioka, H., *Bull. Chem. Soc. Jpn.* **41**, 2840 (1968).
23. Topsøe, N. Y., *Science* **265**, 1217–1219 (1994).
24. Takagi, M., Kawai, T., Soma, M., Onishi, T., and Tamaru, K., *J. Phys. Chem.* **80**, 430 (1976).
25. Nakamoto, K., "Infrared and Raman Spectra of Inorganic and Coordination Compounds," 4th Ed. Wiley, New York, 1986.
26. Weidemann, C., Rehder, D., Kuetgens, U., Hormes, J., and Vilter, H., *Chem. Phys.* **136**, 405 (1989).
27. Poumellec, B., Cortes, R., Sanchez, C., Berthon, J., and Fretigny, C., *J. Phys. Chem. Solids* **54**, 751 (1993).
28. Tullius, T. D., Gillum, W. O., Carlson, R. M. K., and Hodgson, K. O., *J. Am. Chem. Soc.* **102**, 5670 (1980).
29. Glen, G. L., and Dodd, C. G., *J. Appl. Phys.* **39**, 5372 (1968).
30. Lee, P. A., Citrin, P. H., Eisenberger, P., and Kincaid, B. M., *Rev. Mod. Phys.* **53**, 769 (1981).
31. Tachez, M., Theobald, F., Watson, K. J., and Mercier, R., *Acta Crystallogr. B* **35**, 1545 (1979).
32. Richter, E., *Catal. Today* **7**, 93 (1990).
33. Siedlewski, J., *Int. Chem. Eng.* **5**, 297 (1965).
34. Boreskov, G. K., and Rudermann, E. E., *J. Phys. Chem. U.S.S.R.* **14**, 161 (1940).
35. Busca, G., Lietti, L., Ramis, G., and Berti, F., *Appl. Catal. B* **18**, 1–36 (1998).
36. Ramis, G., Busca, G., Bregani, F., and Forzatti, P., *Appl. Catal.* **64**, 259 (1990).
37. Topsøe, N. Y., *J. Catal.* **128**, 499 (1991).
38. Rajadhayaksha, R. A., and Knäzinger, H., *Appl. Catal.* **51**, 81 (1989).
39. Zhu, Z. P., Niu, H. X., Liu, Z. Y., and Liu, S. J., *J. Catal.* **195**, 268 (2000).